

Synthesis, Characterization and Properties of Novel Coumarin Derivatives and Their Europium Complexes

Dong Yan¹ · Dong Li¹ · Guang Cheng¹ · Zehui Yang² · Ling Shi¹ · Dongcai Guo¹

Received: 23 January 2015 / Accepted: 23 March 2015 / Published online: 3 May 2015
© Springer Science+Business Media New York 2015

Abstract Seven novel coumarin derivatives derived from salicylaldehyde and phenol were synthesized and characterized by ¹H NMR and ¹³C NMR spectra, mass spectra, infrared spectra and elemental analysis. Their corresponding Eu(III) complexes having general formula EuL¹⁻⁷(NO₃)₃·2H₂O were successfully prepared and characterized by elemental analysis, EDTA titrimetric, molar conductivity, UV–Vis, FT-IR and thermal performance studies. The luminescence properties, fluorescence quantum yields and the electrochemical properties of the title complexes were investigated. The results showed that the title complexes exhibited characteristic emissions of europium ions and possessed relatively good fluorescence quantum yields. The luminescence intensity of the complex with bromine-substituted group is the strongest among all the title complexes. The introduction of electron-withdrawing groups can increase the luminescence properties and fluorescence quantum yields, decrease the HOMO and LUMO energy levels of the title europium complexes, but electron-withdrawing group conversely. And these title complexes may possibly be useful for studying in luminescent materials field.

Keywords Europium complexes · Coumarin · Synthesis · Electrochemical properties · Luminescence

✉ Dongcai Guo
dcguo2001@163.com

¹ School of Chemistry and Chemical Engineering, Hunan University, Changsha 410082, China

² School of Chemical Engineering, Ningbo University of Technology, Ningbo 315016, China

Introduction

Rare earth organic complexes have attracted significant attention due to their functional optical, electronic and magnetic properties. Their fascinating optical properties make the complexes attractive for multiple applications, such as MRI contrast agents [1, 2], optical amplifiers [3, 4], organic light emitting diodes (OLEDs) [5, 6], probes [7, 8], lasers [9], etc. The luminescence intensity of rare earth complexes is strongly dependent on the efficiency of ligand absorption in the UV region, the efficiency of ligand-to-metal energy transfer, and the efficiency of rare earth luminescence [10], thus the luminescence intensity of rare earth complexes is relationship to central ion and the structure of organic ligand. Therefore, the luminescence excited directly from the rare earth ions is unfavorable and so, it is very important to design and synthesize novel chelating ligands possessing high absorption efficiency and high efficient of ligand-to-RE(III) ions energy transfers. It is well known that coumarin derivatives are one kind of lactone compounds and widely present in nature. They have been reported to possess significant biological activities and pharmacological actions, such as anti-tumor, anti-HIV, anti-oxidation, anti-coagulation, anti-arrhythmic, anti-osteoporosis, analgesic, antibacterial and photosensitivity [11, 12], and widely used in the fields of medicine and pesticides, fluorescent probe [13]. Coumarin derivatives have been extensively studied due to their good planarity and high energy transfer efficiency. The lactone coumarin skeleton of 3-acetyl coumarin possessing good conjugated plane, rigid structure and various coordination sites, so this kind of compounds is usually used as the organic ligand of the rare earth luminescent complexes.

In this paper, seven novel coumarin derivatives and their corresponding europium complexes were synthesized, the luminescent and electrochemical properties of the title complexes were investigated, and the relationship between the

structure of the ligand and the properties of complexes was also explored in detail. The synthesis route for the coumarin derivatives is shown in Scheme 1.

Experimental

Materials

The purity of Eu_2O_3 exceeded 99.99 %, $\text{Eu}(\text{NO}_3)_3$ were prepared according to literature methods [14], chloroacetic acid was of CP grade, phenol derivatives, salicylaldehyde and other reagents were of AR grade, and all used without further purification.

Physical Measurements

The melting points of the synthesized compounds were determined on a TECH XT-4 melting point apparatus and were uncorrected. ^1H NMR and ^{13}C NMR spectra were measured with a Bruker-400 MHz nuclear magnetic resonance spectrometer with deuterated chloroform (CDCl_3) or dimethyl sulfoxide (DMSO)- d_6 as a solvent and TMS as internal reference. The electron impact mass spectra (EI-MS) were measured using a MAT95XP analyzer. Elemental analysis were carried out with a Flash EA1112 elemental analyzer. The UV–Vis spectra were recorded on a LabTech UV-2100 UV-Visible Spectrophotometer and dimethyl sulfoxide (DMSO) was used as a reference and a solvent. The infrared spectra (KBr pellets) were recorded in the region $4000\text{--}400\text{ cm}^{-1}$ on a Shimadzu IRAffinity-1 FT-IR spectrophotometer. Luminescence spectra were monitored by HIACHI F-2700 spectrophotometer at room temperature, the widths of both the excitation and emission slit were 2.5 nm and the voltage of photomultiplier tube was 700 V. Thermal gravimetric (TG) and differential thermal analyses (DTA) were carried out up to $800\text{ }^\circ\text{C}$ with a heating speed of $20\text{ }^\circ\text{C}/\text{min}$ in the static air atmosphere on a SHIM ADZU DTG-60 thermogravimetric analyzer. Cyclic voltammetry (CV) measurements were performed using a CHI 660d electrochemical workstation, the sodium nitrite solution (0.1 M) used as electrolyte, DMSO as solvent. The cyclic voltammogram was recorded at a scan speed of $50\text{ mV}\cdot\text{s}^{-1}$ at a sensitivity of 1 mA.

General Procedure for Synthesis of the Intermediates

Synthesis of 3-acetyl Coumarin (A)

A mixture of salicylaldehyde (0.02 mmol, 2.10 mL), ethyl acetoacetate (0.02 mol, 2.50 mL), absolute ethyl alcohol (50 mL) was placed in a 150 mL three-neck flask, which was heated to reflux under stirring, then several drops of piperidine was added. The mixture was stirred for a further 5 h at

the same temperature. Then, the reaction mixture was cooled to room temperature, the resulting precipitate was collected by filtration and washed several times with hot ethanol [15]. After drying, the product was recrystallized from ethanol and dried under vacuum to give yellow needle crystals (**A**). Yield: 82 %. m.p. $118\text{ }^\circ\text{C}$; ^1H NMR (400 MHz, CDCl_3) δ/ppm 8.51 (s, 1H, CH), 7.68–7.63 (m, 2H, ArH), 7.39–7.34 (m, 2H, ArH), 2.73 (s, 1H, CH_3). MS (EI) m/z (%): 190.1 (M+2, 1), 189.1 (M+1, 7), 188.1 (M, 53), 173.1 (100), 145.1 (15), 89.1 (23).

Synthesis of Phenoxyacetic Acid Derivatives (B^{1–7})

Compounds B^{1-7} were prepared by similar procedures. In a typical synthesis of B^1 , monochloroacetic acid (0.04 mol, 3.78 g) was dissolved in deionized water (15 mL) under the condition of stirring and an ice bath. Then NaOH (25 %) was added dropwise until the pH value was adjusted to 9–10, then a solution of sodium chloroacetate was obtained. To a solution of NaOH (0.03 mol, 1.20 g), deionized water (15 mL) and ethanol (5 mL), phenol (0.04 mol, 3.76 g) was slowly added under stirring. After addition, the mixture was stirred for 20 min, then the above sodium chloroacetate was added dropwise, and heated to $105\text{ }^\circ\text{C}$ and refluxed for 5 h. The reaction mixture was cooled to room temperature. The pH value of the mixture was acidified to 1–2 with diluted hydrochloric acid. The precipitate was filtered, washed with diluted hydrochloric acid many times, and recrystallized and dried in vacuum, resulting in a white solid product of the phenoxyacetic acid (B^1). White crystals. Yield: 76 %. ^1H NMR (CDCl_3) δ/ppm : 7.32 (dd, $J=8.5, 7.6\text{ Hz}$, 2H, ArH), 7.04 (t, $J=7.4\text{ Hz}$, 1H, ArH), 6.94 (d, $J=8.6\text{ Hz}$, 2H, ArH), 4.69 (s, 2H, CH_2); MS (ESI) m/z (%): 304 (2 M, 14), 303 (2 M-1, 100), 151 (M-1, 29).

p-fluorophenoxyacetic acid (B^2). White solid. Yield: 72 %. ^1H NMR (CDCl_3) δ/ppm : 7.00 (d, $J=8.0\text{ Hz}$, 2H, ArH), 6.88 (d, $J=8.0\text{ Hz}$, 2H, ArH), 4.66 (s, 2H, CH_2); MS (EI) m/z (%): 171 (M+1, 10), 170 (M, 100), 125 (77), 112 (42), 95 (69), 75 (16).

p-chlorophenoxyacetic acid (B^3). White solid. Yield: 82 %. ^1H NMR (CDCl_3) δ/ppm : 7.28 (d, $J=8.4\text{ Hz}$, 2H, ArH), 6.86 (d, $J=8.4\text{ Hz}$, 2H, ArH), 4.67 (s, 2H, CH_2); MS (EI) m/z (%): 188 (M+2, 31), 186 (M, 100), 141 (80), 128 (56), 111 (57), 99 (33), 75 (34).

p-bromophenoxyacetic acid (B^4). White solid. Yield: 77 %. ^1H NMR (CDCl_3) δ/ppm : 7.42 (d, $J=9.0\text{ Hz}$, 2H, ArH), 6.81 (d, $J=9.0\text{ Hz}$, 2H, ArH), 4.72 (s, 2H, CH_2); MS (EI) m/z (%): 232 (M+1, 96), 230 (M-1, 100), 187 (46), 185 (48), 174 (35), 172 (36), 157 (41), 155 (38), 143 (18), 76 (21).

p-nitrophenoxyacetic acid (B^5). White crystals. Yield: 68 %. ^1H NMR (400 MHz, $\text{DMSO}-\text{d}_6$) δ/ppm : ^1H NMR (CDCl_3) δ/ppm : 8.21 (d, $J=9.2\text{ Hz}$, 2H, ArH), 7.14 (d, $J=9.2\text{ Hz}$, 2H, ArH), 4.85 (s, 2H, CH_2); MS (EI) m/z (%): 198 (M+1, 11), 197 (M, 100), 181 (5), 167 (18), 152 (86), 139 (12), 122 (23), 109 (37), 92 (30), 76 (19).

p-methoxyphenoxyacetic acid (**B**⁶). White crystals. Yield: 76 %. ¹H NMR (CDCl₃) δ/ppm: 6.90–6.83 (m, 4H, ArH), 4.64 (s, 2H, CH₂), 3.78 (s, 3H, OCH₃); MS (EI) m/z (%): 183 (M+1, 6), 182 (M, 64), 123 (100), 109 (19), 95 (27), 77 (9).

p-methylphenoxyacetic acid (**B**⁷). White crystals. Yield: 71 %. ¹H NMR (CDCl₃) δ/ppm: 7.11 (d, *J*=8.4 Hz, 2H, ArH), 6.83 (d, *J*=8.4 Hz, 2H, ArH), 4.66 (s, 2H, CH₂), 2.31 (s, 3H, CH₃); MS (EI) m/z (%): 167 (M+1, 10), 166 (M, 100), 121 (63), 107 (49), 91 (65), 77 (25), 65 (16).

Synthesis of Ethyl Phenoxyacetate Derivatives (**C**^{1–7})

Compounds (**C**^{1–7}) were prepared by similar procedures. In a typical synthesis of **4a**, a mixture of phenoxyacetic acid (0.02 mol, 3.04 g) and absolute ethanol (40 mL) was added to a 150 mL three-neck flask in an ice bath, then acetyl chloride (1.0 mL) was added dropwise with stirring. The reaction mixture was heated to 80 °C and refluxed for 24 h. The excess solvent was completely removed under reduced pressure on a rotary evaporator. The residue product was used for the next reaction directly without purification.

Synthesis of Phenoxyacetohydrazide Derivatives (**D**^{1–7})

Compounds **D**^{1–7} were prepared by similar procedures. In a typical synthesis of **D**¹, a mixture of phenoxyacetate (10 mmol, 1.80 g), hydrazine hydrate (80 %, 5 mL) and absolute ethanol (30 mL) was added to a 150 mL three-neck flask, then the reaction mixture was refluxed for 5 h. The mixture was cooled to room temperature. The crude product was collected by filtration and washed several times with ethanol. After drying, white needle crystal was recrystallized from ethanol and dried in vacuum.

Phenoxyacetohydrazide (**D**¹). White needle crystals. Yield: 83 %. ¹H NMR (CDCl₃) δ/ppm: 7.80 (s, 1H, NH), 7.36 (t, *J*=7.9 Hz, 2H, ArH), 7.06 (t, *J*=7.4 Hz, 1H, ArH), 6.92 (d, *J*=8.5 Hz, 2H, ArH), 4.60 (s, 2H, CH₂), 3.93 (s, 2H, NH₂); MS (EI) m/z (%): 167 (M+1, 5), 166 (M, 33), 135 (3), 134 (8), 108 (4), 107 (23), 94 (100), 77 (62), 65 (6).

p-fluoro-2-phenoxyacetohydrazide (**D**²). White needle crystals. Yield: 65 %. ¹H NMR (CDCl₃) δ/ppm: 7.72 (s, 1H, NH), 7.02 (d, *J*=8.0 Hz, 2H, ArH), 6.90 (d, *J*=8.0 Hz, 2H, ArH), 4.54 (s, 2H, CH₂), 3.94 (s, 2H, NH₂); MS (EI) m/z (%): 185 (M+1, 3), 184 (21), 169 (2), 126 (5), 125 (24), 112 (100), 97(29), 95 (75), 83 (23), 75 (25), 73 (28).

p-chloro-2-phenoxyacetohydrazide (**D**³). White needle crystals. Yield: 87 %. ¹H NMR (CDCl₃) δ/ppm: 7.72 (s, 1H, NH), 7.31 (d, *J*=9.0 Hz, 2H, ArH), 6.88 (d, *J*=9.0 Hz, 2H, ArH), 4.57 (s, 2H, CH₂), 3.95 (s, 2H, NH₂); MS (EI) m/z (%): 202 (M+2, 7), 200 (M, 21), 143 (6), 141 (17), 130 (33), 128 (100), 111 (35), 99 (4), 77 (7), 65 (5).

p-bromo-2-phenoxyacetohydrazide (**D**⁴). White needle crystals. Yield: 80 %. ¹H NMR (CDCl₃) δ/ppm: 7.69 (s, 1H,

NH), 7.42 (d, *J*=9.0 Hz, 2H, ArH), 6.80 (d, *J*=9.0 Hz, 2H, ArH), 4.55 (s, 2H, CH₂), 3.93 (s, 2H, NH₂); MS (EI) m/z (%): 246 (M+1, 16), 244 (M-1, 16), 187 (16), 185 (18), 174 (97), 172 (100), 157 (49), 155 (46), 145 (8), 143 (8), 106 (7), 93 (11), 77 (18), 65 (24).

p-nitro-2-phenoxyacetohydrazide (**D**⁵). Light yellow crystals. Yield: 78 %. ¹H NMR (CDCl₃) δ/ppm: 8.25 (d, *J*=8.0 Hz, 2H, ArH), 7.63 (s, 1H, NH), 7.02 (d, *J*=8.0 Hz, 2H, ArH), 4.66 (s, 2H, CH₂), 3.94 (s, 2H, NH₂); MS (EI) m/z (%): 212 (M+1, 4), 211 (M, 22), 153 (5), 152 (24), 123 (11), 122 (22), 106 (8), 92 (12), 76 (14), 73 (100), 65 (5).

p-methoxy-2-phenoxyacetohydrazide (**D**⁶). White needle crystals. Yield: 85 %. ¹H NMR (CDCl₃) δ/ppm: 7.72 (s, 1H, NH), 6.90–6.83 (m, 4H, ArH), 4.53 (s, 2H, CH₂), 3.92 (s, 2H, NH₂), 3.77 (s, 3H, OCH₃); MS (EI) m/z (%): 197 (M+1, 4), 196 (M, 30), 138 (2), 137 (9), 124 (100), 109 (28), 107 (16), 92 (11), 77 (17), 64 (6).

p-methyl-2-phenoxyacetohydrazide (**D**⁷). White needle crystals. Yield: 79 %. ¹H NMR (CDCl₃) δ/ppm: 7.75 (s, 1H, NH), 7.12 (d, *J*=8.4 Hz, 2H, ArH), 6.80 (d, *J*=8.4 Hz, 2H, ArH), 4.55 (s, 2H, CH₂), 3.92 (s, 2H, NH₂), 2.30 (s, 3H, CH₃); MS (EI) m/z (%): 181 (M+1, 2), 180 (M, 14), 122 (2), 121 (12), 108 (100), 107 (17), 91 (54), 77 (10), 65 (14).

Synthesis of Coumarin Derivatives (**L**^{1–7})

Compounds **L**^{1–7} were prepared by similar procedures. In a typical synthesis of **L**¹, 3-acetyl coumarin (4 mmol, 0.75 g) was dissolved in 30 mL absolute ethanol in a 150 mL three-neck flask, then phenoxyacetohydrazide (4 mmol, 0.66 g) in 20 mL absolute ethanol was added dropwise with constant stirring and finally heated under reflux for 6 h. A light yellow solid was precipitated, filtered and dried in vacuum. The light yellow crystal was purified by recrystallization from ethyl acetate.

(E)-N'-(1-(2-oxo-2H-chromen-3-yl)ethylidene)-2-phenoxyacetohydrazide (**L**¹). Pale yellow needle crystals. Yield: 71 %. m.p. 132–136 °C; ¹H NMR (400 MHz, CDCl₃) δ/ppm: 9.58 (s, 1H, NH), 8.21 (s, 1H, CH), 7.57 (d, *J*=7.6 Hz, 2H, ArH), 7.32–7.38 (m, 4H, ArH, ArH), 7.08 (m, *J*=7.4 Hz, 1H, ArH), 6.98 (d, *J*=7.9 Hz, 2H, ArH), 4.74 (s, 2H, CH₂), 2.31 (s, 3H, CH₃); ¹³C NMR (100 MHz, CDCl₃) δ/ppm: 164.43, 159.89, 156.79, 154.14, 151.82, 142.67, 132.56, 130.04, 129.52, 129.03, 124.85, 122.71, 118.86, 116.52, 114.68, 67.30, 14.85; IR (KBr) ν/cm⁻¹: 3243, 3053, 1708, 1651, 1611, 1246 736; MS (EI) m/z (%): 338 (M+2, 1), 337 (M+1, 10), 336 (M, 40), 229 (100), 187 (23), 115 (14), 77 (28); Anal. Calcd. for C₁₉H₁₆N₂O₄: C, 67.85; H, 4.79 N, 8.33; O, 19.03. Found: C, 67.83; H, 4.51; N, 8.34.

(E)-2-(4-fluorophenoxy)-N'-(1-(2-oxo-2H-chromen-3-yl)ethylidene)acetohydrazide (**L**²). Yellow crystals. Yield: 72 %. m.p. 143–145 °C; ¹H NMR (400 MHz, CDCl₃) δ/ppm: 9.53 (s, 1H, NH), 8.22 (s, 1H, CH), 7.58 (m, *J*=7.6 Hz, 2H), 7.32–7.38 (m, 2H, ArH), 7.06 (m, *J*=8.3 Hz,

2H, ArH), 6.94 (dd, $J=7.7$, 3.9 Hz, 2H, ArH), 4.71 (s, 2H, CH₂), 2.33 (s, 3H, CH₃); ¹³C NMR (100 MHz, CDCl₃) δ /ppm 164.23, 159.91, 154.15, 152.69, 151.98, 147.57, 142.75, 134.45, 132.62, 129.05, 124.88, 118.85, 116.54, 116.42, 116.01, 68.05, 14.88; IR (KBr) ν /cm⁻¹: 3241, 3053, 1711, 1653, 1613, 1247, 736; MS (EI) m/z (%): 356 (M+2, 1), 355 (M+1, 4), 354 (M, 23), 229 (100), 187 (32), 115 (35), 89 (17), 75 (13), 63 (12); Anal. Calcd. for C₁₉H₁₅FN₂O₄: C, 64.40; H, 4.27, N, 7.91; O, 18.06. Found: C, 67.45; H, 4.32, N, 7.87.

(E)-2-(4-chlorophenoxy)-N'-(1-(2-oxo-2H-chromen-3-yl)ethylidene)acetohydrazide (L³). Yellow crystals. Yield: 70 %. m.p. 157–159 °C; ¹H NMR (400 MHz, CDCl₃) δ /ppm: 9.50 (s, 1H, NH), 8.22 (s, 1H, CH), 7.57–7.59 (m, $J=8.0$ Hz, 2H), 7.36–7.39 (d, $J=11.2$ Hz, 2H, ArH), 7.32–7.34 (m, $J=9.4$ Hz, 2H, ArH), 6.92 (d, $J=7.7$ Hz, 2H, ArH), 4.71 (s, 2H, CH₂), 2.33 (s, 3H, CH₃); ¹³C NMR (100 MHz, CDCl₃) δ /ppm: 163.93, 159.92, 155.38, 154.17, 147.54, 142.72, 132.62, 129.98, 129.42, 129.04, 124.88, 118.84, 116.56, 116.17, 116.02, 67.62, 14.89; IR (KBr) ν /cm⁻¹: 3244, 3065, 1710, 1650, 1613, 1249, 736; MS (EI) m/z (%): 373.1 (M+3, 2), 372.1 (M+2, 7), 370.1 (M, 25), 229.1 (100), 187.1 (27), 141.1 (14), 115.1 (45), 89.1 (21), 75.1 (17), 63.1 (15); Anal. Calcd. for C₁₉H₁₅ClN₂O₄: C, 61.55; H, 4.08 N, 7.56; O, 17.26. Found: C, 61.63; H, 4.06; N, 7.58.

(E)-2-(4-bromophenoxy)-N'-(1-(2-oxo-2H-chromen-3-yl)ethylidene)acetohydrazide (L⁴). Pale yellow crystals. Yield: 68 %. m.p. 165–168 °C; ¹H NMR (400 MHz, CDCl₃) δ /ppm: 9.49 (s, 1H, NH), 8.22 (s, 1H, CH), 7.58–7.60 (m, $J=8.0$ Hz, 2H, ArH), 7.46–7.48 (d, $J=8.2$ Hz, 2H), 7.36–7.38 (m, $J=4.5$ Hz, 2H, ArH), 6.88 (d, $J=8.4$ Hz, 2H), 4.71 (s, 2H, CH₂), 2.33 (s, 3H, CH₃); ¹³C NMR (100 MHz, CDCl₃) δ /ppm: 163.89, 159.87, 155.90, 154.16, 152.03, 142.72, 132.92, 132.62, 132.35, 129.04, 124.88, 118.83, 116.68, 116.49, 115.13, 67.53, 14.90. IR (KBr) ν /cm⁻¹: 3243, 3055, 1713, 1651, 1613, 1246, 744; MS (EI) m/z (%): 418 (M+3, 1), 417 (M+2, 4), 415 (M, 13), 414 (M-1, 15), 229 (100), 215 (23), 187 (33), 115 (38), 89 (17), 76 (12), 63 (13); Anal. Calcd. for C₁₉H₁₅BrN₂O₄: C, 54.96; H, 3.64, N, 6.75; O, 15.41. Found: C, 54.97; H, 3.66; N, 6.73.

(E)-2-(4-nitrophenoxy)-N'-(1-(2-oxo-2H-chromen-3-yl)ethylidene)acetohydrazide (L⁵). Yellow needle crystals. Yield: 72 %. m.p. 160–163 °C; ¹H NMR (400 MHz, DMSO) δ /ppm 11.13 (s, 1H, NH), 8.36 (s, 1H, CH), 8.21 (d, $J=8.5$ Hz, 2H, ArH), 7.81 (d, $J=7.5$ Hz, 1H, ArH), 7.65 (t, $J=7.7$ Hz, 1H, ArH), 7.41–7.44 (dd, $J=15.1$, 7.7 Hz, 2H, ArH), 7.15 (d, $J=8.3$ Hz, 2H, ArH), 5.38 (s, 2H, CH₂), 2.23 (s, 3H, CH₃); ¹³C NMR (101 MHz, DMSO) δ /ppm: 169.65, 164.11, 159.57, 153.87, 147.42, 142.23, 141.40, 132.95, 129.60, 126.84, 126.19, 125.28, 119.32, 116.51, 115.66, 66.35, 16.04. IR (KBr) ν /cm⁻¹: 3245, 3067, 1708, 1651, 1611, 1247, 745; MS (EI) m/z (%): 382 (M+1, 4), 381 (M, 16), 229 (100), 200 (62), 186 (22), 115 (45), 89 (20); Anal. Calcd. for C₁₉H₁₅N₃O₆: C, 59.84; H, 3.96 N, 11.02; O, 25.17. Found: C, 59.87; H, 3.99; N, 10.98.

(E)-2-(4-methoxyphenoxy)-N'-(1-(2-oxo-2H-chromen-3-yl)ethylidene)acetohydrazide (L⁶). Pale yellow needle crystals. Yield: 76 %. m.p. 151–153 °C; ¹H NMR (400 MHz, CDCl₃) δ /ppm: 9.58 (s, 1H, NH), 8.22 (s, 1H, CH), 7.57–7.59 (d, $J=7.7$ Hz, 2H, ArH), 7.39–7.31 (m, 2H, ArH), 6.86–6.93 (m, 4H, ArH), 4.69 (s, 2H, CH₂), 3.80 (s, 3H, OCH₃), 2.32 (s, 3H, CH₃); ¹³C NMR (100 MHz, CDCl₃) δ /ppm: 164.72, 159.90, 155.14, 151.79, 151.07, 150.94, 142.73, 132.58, 129.04, 124.87, 118.86, 116.53, 116.03, 115.81, 115.05, 68.18, 55.72, 14.89; IR (KBr) ν /cm⁻¹: 3246, 3055, 1710, 1649, 1613, 1245, 738; MS (EI) m/z (%): 368 (M+2, 1), 367 (M+1, 7), 366 (M, 28), 200 (100), 171 (13), 115 (37), 89 (15), 63 (16); Anal. Calcd. for C₂₀H₁₈N₂O₅: C, 65.57; H, 4.95 N, 7.65; O, 21.84. Found: C, 65.56; H, 4.91; N, 7.67.

(E)-N'-(1-(2-oxo-2H-chromen-3-yl)ethylidene)-2-(p-tolyloxy)acetohydrazide (L⁷). Pale yellow solid. Yield: 74 %. m.p. 147–150 °C; ¹H NMR (400 MHz, CDCl₃) δ /ppm: 9.57 (s, 1H, NH), 8.22 (s, 1H, CH), 7.57–7.59 (m, $J=7.7$ Hz, 2H, ArH), 7.31–7.38 (m, 2H, ArH), 7.15 (d, $J=8.0$ Hz, 2H, ArH), 6.88 (d, $J=7.9$ Hz, 2H, ArH), 4.71 (s, 2H, CH₂), 2.32 (d, $J=4.9$ Hz, 6H, CH₃); ¹³C NMR (100 MHz, CDCl₃) δ /ppm: 164.65, 159.89, 154.76, 154.13, 151.72, 142.65, 132.54, 130.44, 129.03, 128.76, 126.00, 124.85, 118.86, 116.51, 114.53, 67.52, 20.54, 14.85; IR (KBr) ν /cm⁻¹: 3248, 3058, 1711, 1650, 1612, 1245, 746; MS (EI) m/z (%): 352 (M+2, 2), 351 (M+1, 13), 350 (M, 45), 229 (85), 215 (M, 43), 187 (43), 115 (47), 91 (100), 65 (26); Anal. Calcd. for C₂₀H₁₈N₂O₄: C, 68.56; H, 5.18 N, 8.00; O, 18.27. Found: C, 68.55; H, 5.20; N, 7.96.

Synthesis of the Title Europium Complexes

Synthetic methods of the title europium complexes were similar, so the synthetic process of the complex of compound L¹ was expressed as example. The compound L¹ (0.50 mmol, 0.18 g) was dissolved in 30 mL chloroform in a 100 mL three-neck flask, then 5 mL europium nitrate ethanol solution (0.1 mol·L⁻¹) was added. The pH value of the mixture was adjusted to 6–7 by an aqueous solution of NaOH (1 mol·L⁻¹). The reaction mixture was heated to reflux for 2 h at 60 °C. The precipitated mixture was collected by filtration, and washed several times with chloroform, and then dried in drying oven for 8 h to give complex with ligand L¹. The general synthesis procedures of other complexes with ligands L^{2–7} are similar to that of complex with ligand L¹.

Results and Discussion

Composition and Physical Properties of the Complexes

Analytical data for the newly synthesized title complexes are given in Table 1. Compounds L^{1–7} were easily dissolved in chloroform, DMSO, DMF, acetone and dichloromethane, but

Table 1 The elemental analysis and molar conductance data of the europium complexes

Complexes	Found (calculated) (%)				Λ_m ($S \cdot m^2 \cdot mol^{-1}$)
	C	H	N	Eu	
$EuL^1(NO_3)_3 \cdot 2H_2O$	31.70 (32.11)	2.93 (2.82)	9.80 (9.86)	21.15 (21.41)	16
$EuL^2(NO_3)_3 \cdot 2H_2O$	30.84 (31.32)	2.78 (2.61)	9.48 (9.61)	20.48 (20.88)	20
$EuL^3(NO_3)_3 \cdot 2H_2O$	30.12 (30.60)	2.72 (2.55)	9.25 (9.40)	20.05 (20.40)	18
$EuL^4(NO_3)_3 \cdot 2H_2O$	28.37 (28.90)	2.53 (2.41)	8.81 (8.87)	19.00 (19.26)	12
$EuL^5(NO_3)_3 \cdot 2H_2O$	29.78 (30.20)	2.66 (2.52)	11.02 (11.12)	19.75 (20.13)	25
$EuL^6(NO_3)_3 \cdot 2H_2O$	32.01 (32.43)	3.15 (2.97)	9.28 (9.46)	20.11 (20.54)	17
$EuL^7(NO_3)_3 \cdot 2H_2O$	32.85 (33.15)	3.21 (3.04)	9.55 (9.67)	20.58 (20.99)	22

hardly dissolved in ethanol, methanol and cyclohexane, while the title Eu(III) complexes were only dissolved in DMSO and DMF.

The results of elemental analyses are in good agreement with the theoretical values calculated, indicating that the composition of the seven novel europium complexes conformed to $EuL^{1-7}(NO_3)_3 \cdot 2H_2O$. The molar conductivity values of the title complexes in DMF are lower than that of 1:1 electrolytes ($65-90 S \cdot cm^2 \cdot mol^{-1}$), indicating that all the europium nitrate complexes conformed to a kind of nonelectrolyte [16].

UV Spectra

The UV spectra of the ligands and their corresponding europium complexes were carried out in the DMSO solution ($10^{-4} mol \cdot L^{-1}$), the numerical values of the maximum absorption wavelength (λ) and the molar absorptivities (ϵ) [17] are shown in Table 2. Since the UV spectra of all the complexes exhibit the similar features, only the UV spectra of

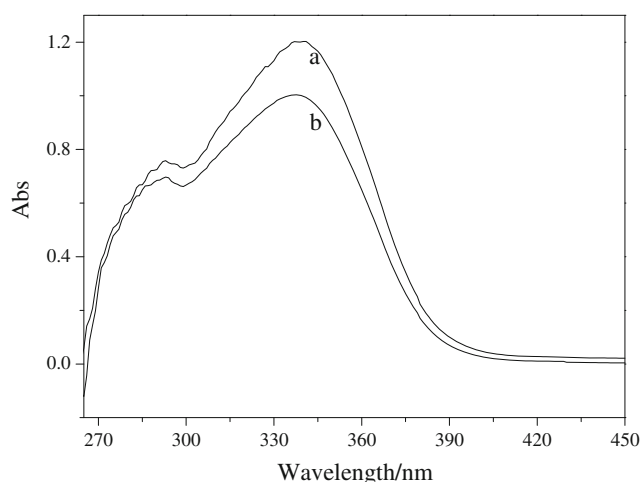
Table 2 The UV data of the europium complexes and ligands in DMSO solution ($10^{-4} mol \cdot L^{-1}$)

Compounds	λ_1 (nm)	$\epsilon_1 (1.0 \times 10^4)$ $L \cdot mol^{-1} \cdot cm^{-1}$	λ_2 (nm)	$\epsilon_2 (1.0 \times 10^4)$ $L \cdot mol^{-1} \cdot cm^{-1}$
L^1	296	0.74	335	1.08
$EuL^1(NO_3)_3 \cdot 2H_2O$	299	0.81	337	1.16
L^2	296	0.67	336	1.00
$EuL^2(NO_3)_3 \cdot 2H_2O$	299	0.74	338	1.19
L^3	297	0.80	336	1.07
$EuL^3(NO_3)_3 \cdot 2H_2O$	299	0.86	339	1.13
L^4	296	0.78	335	1.10
$EuL^4(NO_3)_3 \cdot 2H_2O$	298	0.89	338	1.19
L^5	296	0.71	335	1.10
$EuL^5(NO_3)_3 \cdot 2H_2O$	298	0.76	338	1.21
L^6	296	0.88	336	1.01
$EuL^6(NO_3)_3 \cdot 2H_2O$	298	0.99	338	1.10
L^7	297	0.78	336	1.07
$EuL^7(NO_3)_3 \cdot 2H_2O$	299	1.01	338	1.21

$EuL^2(NO_3)_3 \cdot 2H_2O$ and $EuL^4(NO_3)_3 \cdot 2H_2O$ as well as their corresponding ligands are shown in Figs. 1 and 2, respectively.

In Figs. 1 and 2, the absorption of L^2 and L^4 were characterized by two main absorption bands in the regions 280–350 nm. The ultraviolet absorption spectra of L^2 and L^4 exhibited two peaks at 296 nm, 336 nm and 296 nm, 335 nm, respectively, which were assigned to the $\pi \rightarrow \pi^*$ transition of aromatic ring and $n \rightarrow \pi^*$ transition of conjugation between the lone pair of electrons of p-orbital of N-atom in $C=N$ [18].

The UV spectra of the complexes $EuL^2(NO_3)_3 \cdot 2H_2O$ and $EuL^4(NO_3)_3 \cdot 2H_2O$ show the characteristic absorption of their free ligands, which suggests that the coordination of europium ion does not have a significant influence on the $\pi \rightarrow \pi^*$ and $n \rightarrow \pi^*$ state energy, and also reveals that the absorption of the europium complexes is mainly attributed to the ligands, this maybe due to the f-f transitions are Laporte-forbidden and very weak in nature [19]. But there are certain changes both in frequencies and intensities. The peaks of $EuL^2(NO_3)_3 \cdot 2H_2O$ and $EuL^4(NO_3)_3 \cdot 2H_2O$ appear at 299 nm, 338 nm and 298 nm, 338 nm are slightly shifted to lower frequencies compared to that of free ligands. The modifications of the shifts confirmed the coordination of the ligands to the europium ions.

**Fig. 1** The UV-Visible spectra of $EuL^2(NO_3)_3 \cdot 2H_2O$ (a) and L^2 (b)

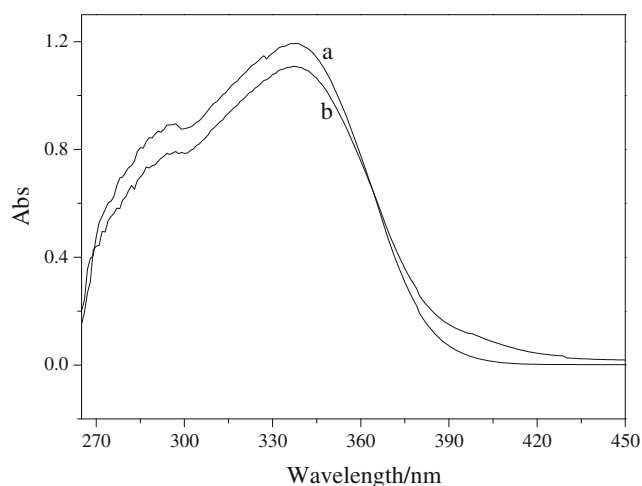


Fig. 2 The UV-Visible spectra of $\text{EuL}^4(\text{NO}_3)_3 \cdot 2\text{H}_2\text{O}$ (a) and L^4 (b)

Thermogravimetric Analysis

The thermal behaviour of the title europium complexes were investigated by thermal analysis. The thermogravimetric (TG) and differential thermal analysis (DTA) was carried out in air atmosphere from ambient temperature up to 800 °C. All the TG-DTA data of the title complexes are listed in Table 3. The TG-DTA curves give the similar thermal decomposition behavior, only the TG-DTA curve of the complex $\text{EuL}^6(\text{NO}_3)_3 \cdot 2\text{H}_2\text{O}$ is selected for illustration as an example (Fig. 3).

From Fig. 3, it shows that the first mass loss occurs between 40 and 200 °C (observed 4.82 %, calc. 4.87 %), and the DTA curve shows a small endothermic peak at 197 °C. The result was coincided with the release of two crystal water molecules. Then, the mass loss between 250 and 280 °C is 49.30 %, and this value is consistent with the calculated value 49.46 % of organic ligand decomposition. In addition, there are two successive exothermic peaks at 358 and 485 °C, and the weight loss ratio of residue is 21.83 %, corresponding to the loss of internally three nitrate molecules. Further heating two complexes to 800 °C, the weight ratio of residues was 24.35 %, the values basically agree with calculated 23.78 %, corresponding to the formation of Eu_2O_3 . The thermal analysis results demonstrate that the title complexes have a satisfactory thermal stability.

Table 3 The thermogravimetric data of the europium complexes

Complexes	Endothermic peak (°C)	Exothermic peak (°C)	Residue (%) Found (Calcd.)
$\text{EuL}^1(\text{NO}_3)_3 \cdot 2\text{H}_2\text{O}$	68, 196	211, 387, 521	24.27 (24.78)
$\text{EuL}^2(\text{NO}_3)_3 \cdot 2\text{H}_2\text{O}$	67, 187	211, 382, 551	24.36 (24.17)
$\text{EuL}^3(\text{NO}_3)_3 \cdot 2\text{H}_2\text{O}$	73, 195	219, 385, 532	23.91 (23.62)
$\text{EuL}^4(\text{NO}_3)_3 \cdot 2\text{H}_2\text{O}$	67, 200	223, 390, 510	24.32 (22.30)
$\text{EuL}^5(\text{NO}_3)_3 \cdot 2\text{H}_2\text{O}$	63, 158	250, 405	25.26 (23.31)
$\text{EuL}^6(\text{NO}_3)_3 \cdot 2\text{H}_2\text{O}$	67, 197	271, 358, 485	24.35 (23.78)
$\text{EuL}^7(\text{NO}_3)_3 \cdot 2\text{H}_2\text{O}$	65, 183	249, 361, 437, 482	25.14 (24.31)

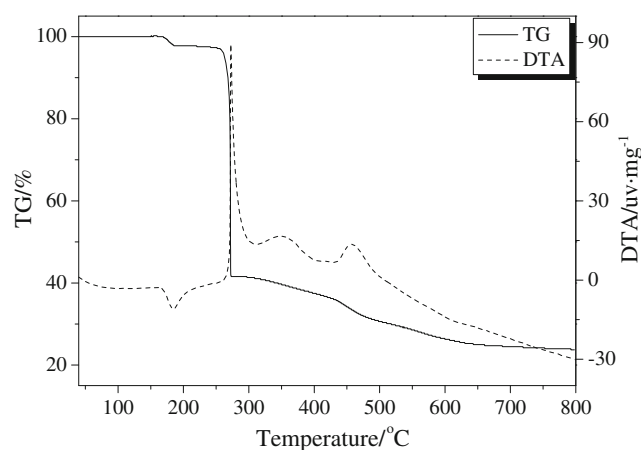


Fig. 3 TG-DTA curves of the complex $\text{EuL}^6(\text{NO}_3)_3 \cdot 2\text{H}_2\text{O}$

FT-IR Spectra

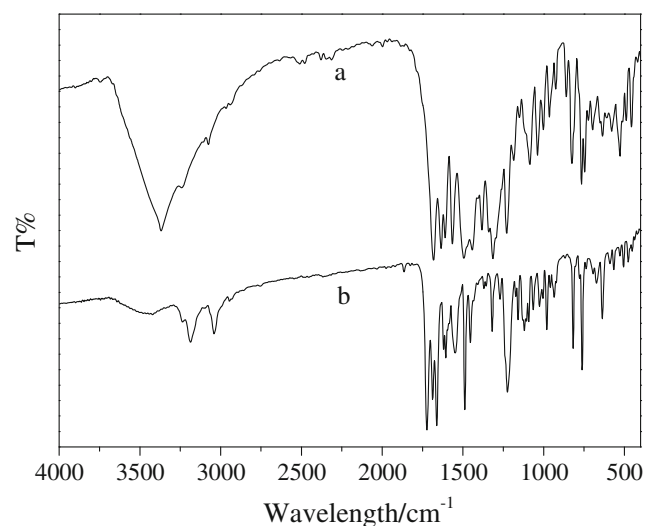
The IR spectral data for the title europium complexes and their corresponding ligands L^{1-7} are listed in Table 4. IR spectra of all the Eu(III) complexes display the same manner, only the IR spectra of $\text{EuL}^3(\text{NO}_3)_3 \cdot 2\text{H}_2\text{O}$ as well as its corresponding ligand are selected for illustration in Fig. 4.

Figure 4 shows that the IR spectrum of the Eu(III) complex is different from its corresponding ligand. The IR spectrum of the free ligand L^3 shows a band at 1710 cm^{-1} , which can be assigned to $\nu(\text{C}=\text{O})$ of the lactone group of coumarin. The bands at 1654 cm^{-1} and 1613 cm^{-1} are attributed to the $\nu(\text{N}-\text{C}=\text{O})$ and $\nu(\text{C}=\text{N})$ of hydrazide group. In the IR spectra of the complex $\text{EuL}^3(\text{NO}_3)_3 \cdot 2\text{H}_2\text{O}$, the bands for $\nu(\text{C}=\text{O})$ shifted to 1668 cm^{-1} ($\Delta\nu=42 \text{ cm}^{-1}$), which indicates that the oxygen atom of $\text{C}=\text{O}$ group in lactone takes part in coordination to the Eu(III) ions. Further, the absorption peaks of $\nu(\text{N}-\text{C}=\text{O})$ and $\nu(\text{C}=\text{N})$ red shift upfield by 28 cm^{-1} and 29 cm^{-1} , respectively, it suggest that Eu(III) ions bonded with the oxygen atom of $\text{N}-\text{C}=\text{O}$ and nitrogen atom of $\text{C}=\text{N}$. However, the $\nu(\text{Ar}-\text{O}-\text{C})$ absorption band appears at around 1249 cm^{-1} and remains unchanged. This is due to the poor coordination ability of $\text{Ar}-\text{O}-\text{C}$ and the free ligand's large sterically hindered effect, which prevents oxygen atom of $\text{Ar}-\text{O}-\text{C}$ group from coordinating to Eu(III) ions. The absorption bands lying at 1480 cm^{-1} and 1317 cm^{-1} are observed in the complex,

Table 4 IR spectral data of the ligands and their europium complexes

Compounds	lactone	hydrazide		$\nu_{\text{Ar-O-C}}$	$\nu_{\text{N-H}}$	$\nu_{\text{O-H}}$	$\nu_{\text{NO}_3^-}$
	$\nu_{\text{C=O}}$	$\nu_{\text{C=O}}$	$\nu_{\text{C=N}}$				
L ¹	1708	1651	1611	1246	3243	–	
EuL ¹ (NO ₃) ₃ ·2H ₂ O	1662	1623	1587	1245	3240	3411	1480,1325,1026,819
L ²	1711	1653	1613	1247	3241	–	
EuL ² (NO ₃) ₃ ·2H ₂ O	1663	1622	1585	1244	3238	3415	1481,1322,1028,823
L ³	1710	1650	1613	1249	3244	–	
EuL ³ (NO ₃) ₃ ·2H ₂ O	1668	1622	1584	1247	3243	3411	1480,1317,1026,818
L ⁴	1713	1651	1613	1246	3243	–	
EuL ⁴ (NO ₃) ₃ ·2H ₂ O	1666	1624	1583	1246	3241	3419	1483,1320,1024,815
L ⁵	1708	1651	1611	1247	3245	–	
EuL ⁵ (NO ₃) ₃ ·2H ₂ O	1664	1633	1584	1245	3241	3417	1479,1305,1028,830
L ⁶	1710	1649	1613	1245	3246	–	
EuL ⁶ (NO ₃) ₃ ·2H ₂ O	1658	1623	1587	1243	3246	3405	1486,1321,1026,819
L ⁷	1711	1650	1612	1245	3248	–	
EuL ⁷ (NO ₃) ₃ ·2H ₂ O	1666	1623	1587	1243	3243	3409	1490,1306,1031,816

which is attributed the asymmetric vibration absorption (ν_{as}) and symmetric vibration absorption (ν_{s}). The frequency separation [$\Delta\nu=|\nu_1-\nu_4|$] between the asymmetric and symmetric stretching of this group can be made to distinction between these binding states. The difference between the two strongest absorption bands of the nitrate groups ($|\nu_1-\nu_4|$) can be defined as $\Delta\nu$. It is generally believed that the $\Delta\nu$ value is below 200 for the bidentate nitrate moiety, but above 200 for the monodentate nitrate moiety [20]. The difference between ν_1 and ν_4 of EuL³(NO₃)₃·2H₂O is approximately 163 cm⁻¹, which can be suggested that the coordinated NO₃⁻ ions in the europium complexes are bidentate coordination. The coordination is further confirmed through the appearance of two medium intensity bands

**Fig. 4** The IR spectra of EuL³(NO₃)₃·2H₂O (a) and L³ (b)

around 526 cm⁻¹ and 430 cm⁻¹ assigned to Eu-O and Eu-N stretching vibrations [21].

The IR spectrum of the complex exhibits a broad band at 3411 cm⁻¹, indicating that lattice water molecules are existent in the molecular unit of complexes, which is in agreement with the elemental analysis and thermogravimetric analysis discussed in the previous section. So we propose the most probable coordination structure of the europium complexes of the ligands shown in Fig. 5.

Luminescence Properties

The luminescence spectra for the solid complexes EuL¹⁻⁷(NO₃)₃·2H₂O were measured at room temperature under a drive voltage of 700 V, and excitation and emission slit widths were both 2.5 nm. The luminescence spectral data of the title complexes are listed in Table 5. Since the luminescence spectra of all the complexes are similar, only the luminescence spectrum of EuL⁴(NO₃)₃·2H₂O is selected for illustration, and the excitation spectra and emission spectra are shown in Fig. 6.

As shown in Table 5, all complexes present the characteristic luminescence of europium ions, and there is no trace emission from ligands in the complexes, indicating that the ligands are comparatively organic chelators to sensitize luminescence of Eu(III) ions. It is shown in Fig. 6 that the maximum excitation wavelength of the complex EuL⁴(NO₃)₃·2H₂O is observed at 370 nm, due to the $\pi \rightarrow \pi^*$ transition centered at the ligand L⁴. The complex appears emission bands at 595, 620 nm with the characteristic properties of europium ions, which are assigned to $^5\text{D}_0 \rightarrow ^7\text{F}_1$ and $^5\text{D}_0 \rightarrow ^7\text{F}_2$ transitions, respectively. The $^5\text{D}_0 \rightarrow ^7\text{F}_1$ transition is a magnetic transition, which is less affected by the free ligand, and is

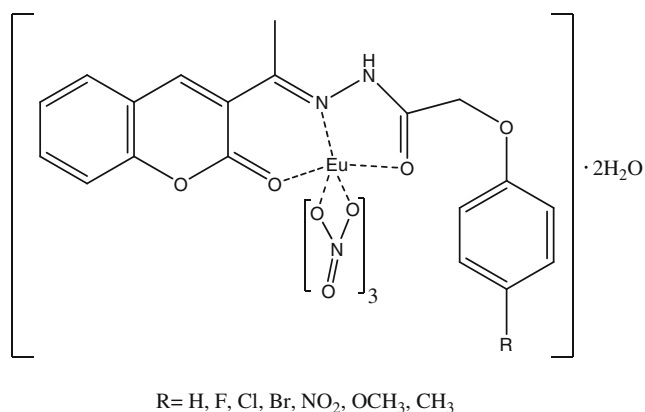


Fig. 5 The most probable coordination structure of the complexes

irrelevant to the symmetry of rare earth ions. In the process of coordination, ligand field environment has a significant impact on the $^5D_0 \rightarrow ^7F_2$ transition (electric dipole transition), which is closely related to the symmetry of the ligand field. It can be observed that the intensity of the hypersensitive $^5D_0 \rightarrow ^7F_2$ transition is greater than that of the $^5D_0 \rightarrow ^7F_1$ transition and the former is about 3.78 times higher than the latter, which suggests that europium ion do not lie in a centrosymmetric coordination site [22]. The asymmetric microenvironment causes the polarization of the Eu(III) ions under the influence of electric field of the surrounding ligands, which increases the probability for the electric dipole transition [23]. Additionally, this typical narrow and sharp emission peak of Eu(III) ions can be detected at 620 nm, indicating that the complex has good monochromaticity and the energy transferred from the excited triplet state of the ligand to the vibrational state of the europium ion is efficient [24].

By comparison of the luminescence excitation spectra and the UV absorption spectroscopy of the title europium complexes, their absorption peak position and shape change a lot. The reason may be that some electrons of complexes molecular of triplet triplet state (T_1) crossing to the triplet state and then back to the ground state, thus the number of electrons directly from the excited state back to the ground state is decreased. The shape of the luminescence excitation spectra

Table 5 The fluorescence spectra data of the europium complexes

Complexes	λ_{ex}/nm	$^5D_0 \rightarrow ^7F_1$		$^5D_0 \rightarrow ^7F_2$	
		λ_{em}/nm	I/a.u.	λ_{em}/nm	I/a.u.
EuL ¹ (NO ₃) ₃ ·2H ₂ O	370	595	525.5	6202	2176.3
EuL ² (NO ₃) ₃ ·2H ₂ O	368	595	631.5	619	2195.7
EuL ³ (NO ₃) ₃ ·2H ₂ O	370	594	1316.1	619	4875.2
EuL ⁴ (NO ₃) ₃ ·2H ₂ O	371	595	2100.3	620	7944.3
EuL ⁵ (NO ₃) ₃ ·2H ₂ O	370	595	794.5	620	3041.8
EuL ⁶ (NO ₃) ₃ ·2H ₂ O	371	595	456.5	620	1607.6
EuL ⁷ (NO ₃) ₃ ·2H ₂ O	369	595	313.7	619	1143.5

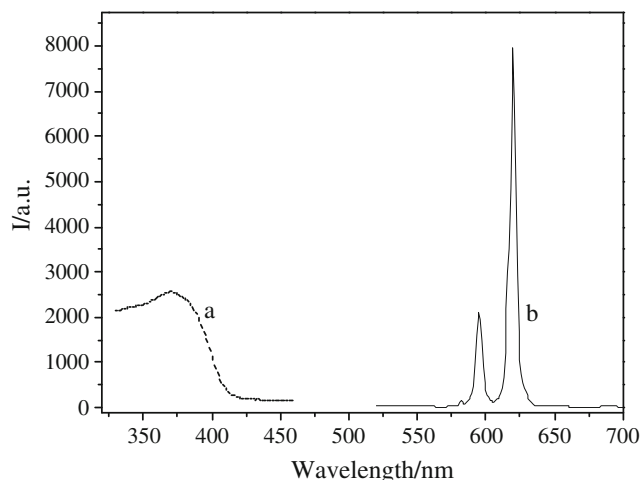


Fig. 6 The excitation spectrum (a) and emission spectrum (b) of EuL⁴(NO₃)₃·2H₂O

will be affected, resulting in that is not completely consistent with the form of ultraviolet absorption spectra.

The intensity of the intra-molecular energy transfer between the triplet levels of the ligand and the emitting level of europium ions is one of the key factors influencing the luminescence properties of lanthanide complexes (Antenna effect). From Table 5, compared with unsubstituted complex EuL¹(NO₃)₃·2H₂O, the luminescence intensities of the complexes with electron-withdrawing groups (F, Cl, Br, NO₂) are much more stronger, and the luminescence intensities of the complexes with electron-donating groups (OCH₃, CH₃) are decreased. Among the title complexes EuL¹⁻⁷(NO₃)₃·2H₂O, the luminescence intensity of the complex EuL⁴(NO₃)₃·2H₂O was the highest, which indicated that the triplet level of ligand L⁴ was in an appropriate level to center the Eu(III) ion and the energy transition from ligand L⁴ to the Eu(III) ion was easier than with the other ligands. However, the luminescence intensities of EuL⁶⁻⁷(NO₃)₃·2H₂O were rather weaker, this was because too small the energy levels difference that caused the energy back to the triplet state of the ligands. All the above analyses confirmed that the ligand L⁴ was more suitable than another ligands to transfer energy to the lowest excited state level of the Eu(III) ion.

Fluorescence Quantum Yield Studies

The fluorescence quantum yields (Φ_{fx}) of the title europium complexes were determined by the reference method and calculated by the following equation [25]:

$$\Phi_{fx} = \frac{n_x^2}{n_{std}^2} \cdot \frac{F_x}{F_{std}} \cdot \frac{A_{std}}{A_x} \cdot \Phi_{fstd}$$

In the formula, subscripts std and x refer to the standard and the unknown, respectively, Where, n_x and the n_{std} are the refractive indices of sample and standard ($n_x=1.480$, $n_{std}=1.337$),

respectively. F is the area of fluorescence integral, and A is the absorbance at the exciting wavelength of UV absorption. Both the sample and standard are excited at the same relevant wavelength, so that the A_{std} is equivalent to A_x . The fluorescence spectral data of $\text{EuL}^{1-7}(\text{NO}_3)_3 \cdot 2\text{H}_2\text{O}$ were measured at room temperature in DMSO (10^{-6} M) solution with excitation and emission slit widths were 5.0 nm, and the calculated results of Φ_{fx} of the title complexes are listed in Table 6.

As shown in Table 6, the change rule of the luminescence intensities of different complexes recorded in solid is consistent with that in liquid, and the same as the data of fluorescence quantum yields. The fluorescence quantum yields of $\text{EuL}^{2-5}(\text{NO}_3)_3 \cdot 2\text{H}_2\text{O}$ with electron-withdrawing groups (F, Cl, Br, NO_2) are higher than that of $\text{EuL}^1(\text{NO}_3)_3 \cdot 2\text{H}_2\text{O}$, and halogen-containing complexes show higher fluorescence quantum yields, $\text{EuL}^4(\text{NO}_3)_3 \cdot 2\text{H}_2\text{O}$ shows the highest quantum yield (0.562), which is due to the fact that L^4 possesses the stronger p - π conjugation effect compared with L^3 and L^2 , and the triplet energy level of bromine-substituted ligand matches better to the excited state level of Eu(III). On the contrary, the introduction of the electron-donating group (CH_3 , OCH_3) in the ligands can decrease the fluorescence quantum yields of the complexes $\text{EuL}^{6-7}(\text{NO}_3)_3 \cdot 2\text{H}_2\text{O}$, and the fluorescence quantum yield of the complex with methyl substituent is the lowest 0.259. The reason is that the electron density of the phenyl rings increases with improvement of the triplet energy level of free ligands, so the energy gap between the triplet energy level and the excited state level of Eu(III) became larger. From the above discussions, we conclude that all the title complexes $\text{EuL}^{1-7}(\text{NO}_3)_3 \cdot 2\text{H}_2\text{O}$ possess relatively good fluorescence quantum yields.

Electrochemical Properties

To study the electrochemical properties of the title europium complexes, cyclic voltammetry (CV) experiments were conducted in DMSO solution and the oxidation potential E_{OX} of the complexes were measured. The HOMO and LUMO energy levels are calculated using equations $E_{\text{HOMO}} = 4.74 + eE_{\text{OX}}$, $E_{\text{LUMO}} = E_{\text{HOMO}} - E_{\text{g}}$, $E_{\text{g}} = 1240/\lambda_{\text{onset}}$ (eV), where λ_{onset} was the starting value of the largest UV-Vis absorption spectra peak [26]. The electrochemical data of the complexes are

Table 6 The fluorescence quantum yields of the europium complexes

Complexes	λ_{ex} (nm)	I (a.u.)	Φ_{fx}
$\text{EuL}^1(\text{NO}_3)_3 \cdot 2\text{H}_2\text{O}$	310	851	0.466
$\text{EuL}^2(\text{NO}_3)_3 \cdot 2\text{H}_2\text{O}$	311	868	0.471
$\text{EuL}^3(\text{NO}_3)_3 \cdot 2\text{H}_2\text{O}$	309	1322	0.536
$\text{EuL}^4(\text{NO}_3)_3 \cdot 2\text{H}_2\text{O}$	312	1638	0.562
$\text{EuL}^5(\text{NO}_3)_3 \cdot 2\text{H}_2\text{O}$	312	933	0.493
$\text{EuL}^6(\text{NO}_3)_3 \cdot 2\text{H}_2\text{O}$	311	535	0.318
$\text{EuL}^7(\text{NO}_3)_3 \cdot 2\text{H}_2\text{O}$	310	511	0.259

Table 7 The E_{HOMO} , E_{LUMO} and E_{g} of the europium complexes

Complexes	λ_{onset} (nm)	E_{OX} (V)	E_{HOMO} (eV)	E_{g} (eV)	E_{LUMO} (eV)
$\text{EuL}^1(\text{NO}_3)_3 \cdot 2\text{H}_2\text{O}$	297	0.701	5.441	4.175	1.266
$\text{EuL}^2(\text{NO}_3)_3 \cdot 2\text{H}_2\text{O}$	296	0.679	5.419	4.189	1.230
$\text{EuL}^3(\text{NO}_3)_3 \cdot 2\text{H}_2\text{O}$	298	0.685	5.425	4.161	1.264
$\text{EuL}^4(\text{NO}_3)_3 \cdot 2\text{H}_2\text{O}$	296	0.693	5.433	4.189	1.244
$\text{EuL}^5(\text{NO}_3)_3 \cdot 2\text{H}_2\text{O}$	298	0.667	5.407	4.161	1.246
$\text{EuL}^6(\text{NO}_3)_3 \cdot 2\text{H}_2\text{O}$	297	0.709	5.449	4.175	1.274
$\text{EuL}^7(\text{NO}_3)_3 \cdot 2\text{H}_2\text{O}$	298	0.712	5.452	4.161	1.291

summarized in Table 7 and the cyclic voltammetry curve of $\text{EuL}^1(\text{NO}_3)_3 \cdot 2\text{H}_2\text{O}$ is depicted in the Fig. 7.

As shown in Table 7, the oxidation potential and HOMO and LUMO energy levels of $\text{EuL}^{2-5}(\text{NO}_3)_3 \cdot 2\text{H}_2\text{O}$ are lower than that of $\text{EuL}^1(\text{NO}_3)_3 \cdot 2\text{H}_2\text{O}$. The reason is that the introduction of electron-withdrawing groups can reduce the electron cloud density on the benzene ring, weaken the betatopic ability of the title complexes, thus the oxidation potential reduced. The HOMO energy levels and the oxidation potential of halogen atom-substituted europium complexes are determined in the following order: $\text{F} < \text{Cl} < \text{Br}$. The oxidation potential and HOMO and LUMO energy levels of $\text{EuL}^{6-7}(\text{NO}_3)_3 \cdot 2\text{H}_2\text{O}$ are higher than that of $\text{EuL}^1(\text{NO}_3)_3 \cdot 2\text{H}_2\text{O}$, this stems from the fact that the introduction of electron-donating group will increase oxidation potential. The energy gap of europium complexes range from 4.161 to 4.189 eV, which indicates that the electron-donating groups and electron-withdrawing groups have no apparent effect on energy gap. However, the substituent type of the title complexes has a certain degree of influence on E_{OX} , HOMO and LUMO energy levels. According to the discussion above, the introduction of electron-

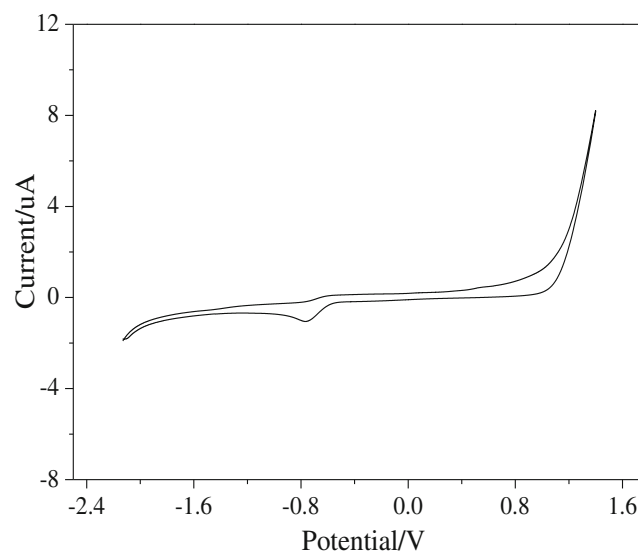


Fig. 7 The CV curve of $\text{EuL}^2(\text{NO}_3)_3 \cdot 2\text{H}_2\text{O}$

withdrawing groups tend to decrease the HOMO and LOMO energy levels, and the oxidation potential of the complexes the introduction of electron-donating groups can increase the HOMO and LOMO energy levels, and the oxidation potential of the complexes.

Conclusions

Seven new coumarin derivatives have been designed and synthesized by the means of Perkin reaction, substitution, esterification, hydrazine through the starting material salicylic aldehyde, ethyl acetoacetate and phenol derivatives, and formed a series of stable solid complexes with europium ions. The coordination of the ligands to Eu(III) ions was occurring at one oxygen atom of the coumarin, one nitrogen atom and one oxygen atom of acyl hydrazone. Thermal study indicates that title europium complexes are thermally stable. The luminescent test results revealed that all the title Eu(III) complexes emitted characteristic luminescence of Eu(III) ions and the complex of the ligand with bromo-substituted group possesses the strongest luminescence intensity and the highest fluorescence quantum yield among all the title complexes. The introduction of electron-donating groups to the ligands can increase the HOMO and LOMO energy levels, the oxidation potential of the title Eu(III) complexes. However, the result of introduction of electron-withdrawing groups was just opposite. These results demonstrate that the title complexes are expected to be used as luminescent materials in various fields.

Acknowledgments The authors are grateful for the financial support of the National Natural Science Foundation of China (No.J1103312; No.J1210040; No.21341010), the Innovative Research Team in University (No.IRT1238) and chemical excellent engineer training program of Hunan university. We also thank Dr. William Hickey, the U.S. professor of HRM, for the English editing on this paper.

References

- Zhou J, Lu ZG, Shan GG, Wang SH, Liao Y (2014) Gadolinium complex and phosphorescent probe-modified NaDyF₄ nanorods for T₁- and T₂-weighted MRI/CT/phosphorescence multimodality imaging. *Biomaterials* 35:368–377
- Mishra A, Fouskova P, Angelovski G, Balogh E, Mishra AK, Logothetis NK, Tóth É (2008) Facile synthesis and relaxation properties of novel bispolyazamacrocyclic Gd³⁺ complexes: an attempt towards calcium-sensitive MRI contrast agents. *Inorg Chem* 47:1370–1381
- Feng J, Zhang HJ (2013) Hybrid materials based on lanthanide organic complexes: a review. *Chem Soc Rev* 42:387–410
- Suzuki H, Hattori Y, Iizuka T, Yuzawa K, Matsumoto N (2003) Organic infrared optical materials and devices based on an organic rare earth complex. *Thin Solid Films* 438:288–293
- Wei HB, Yu G, Zhao ZF, Liu ZW, Bian ZQ, Huang CH (2013) Constructing lanthanide [Nd (III), Er (III) and Yb (III)] complexes using a tridentate N, N, O-ligand for near-infrared organic light-emitting diodes. *Dalton Trans* 42:8951–8960
- Oyamada T, Kawamura Y, Koyama T, Sasabe H, Adachi C (2004) Formation of europium chelate complexes by vacuum co-deposition and their application in organic light-emitting diodes. *Adv Mater* 16:1082–1086
- Wang Y, Ji L, Zhang B, Yin P, Qiu Y, Song D, Zhou J, Li Q (2013) Upconverting rare-earth nanoparticles with a paramagnetic lanthanide complex shell for upconversion fluorescent and magnetic resonance dual-modality imaging. *Nanotechnology* 24:175101
- Yang CL, Xu J, Li JY, Lu MG, Li YB, Wang XL (2014) An efficiently colorimetric and fluorescent probe of fluoride, acetate and phosphate ions based on a novel trinuclear Eu-complex. *Sensors Actuators B Chem* 196:133–139
- Sun LN, Zhang HJ, Meng QG, Liu FY, Fu LS, Peng CY, Yu JB, Zheng GL, Wang SB (2005) Near-infrared luminescent hybrid materials doped with lanthanide (Ln) complexes (Ln = Nd, Yb) and their possible laser application. *J Phys Chem B* 109:6174–6182
- Wang W, Huang Y, Tang N (2007) Synthesis and infrared and fluorescence spectra of rare earth complexes with a novel amide-based ligand. *Spectrochim Acta A* 66:1058–1062
- Yadav P, Satapathi S, Kumari M, Chaturvedi A, Li L, Samuelson LA, Kumar J, Sharma SK (2014) Synthesis of two-photon active cinnamoyl coumarins for high-contrast imaging of cancer cells and their photophysical characterization. *J Photochem Photobiol A Chem* 280:39–45
- Amin KM, Abdel Gawad NM, Abdel Rahman DE, el Ashry MKM (2014) New series of 6-substituted coumarin derivatives as effective factor Xa inhibitors: Synthesis, in vivo antithrombotic evaluation and molecular docking. *Bioorg Chem* 52:31–43
- Mahapatra AK, Hazra G, Roy J, Sahoo P (2011) A simple coumarin-based colorimetric and ratiometric chemosensor for acetate and a selective fluorescence turn-on probe for iodide. *J Lumin* 131:1255–1259
- Nakagawa K, Amita K, Mizuno H, Inoue Y, Hakushi T (1987) Preparation of some lanthanoid picrates and the behavior of their water of hydration. *Bull Chem Soc Jpn* 60:2037
- Li J, Li X, Wang S (2012) Synthesis, photoluminescent behaviors, and theoretical studies of two novel ketocoumarin derivatives. *Spectrochim Acta, Part A* 88:31–36
- Geary WJ (1971) The use of conductivity measurements in organic solvents for the characterisation of coordination compounds. *Coord Chem Rev* 7:81–122
- Feigenbrugel V, Loew C, Calve TL, Mirabel P (2005) Near-UV molar absorptivities of acetone, alachlor, metolachlor, diazinon and dichlorvos in aqueous solution. *J Photochem Photobiol A Chem* 174:76–81
- Gansow OA, Loeffler PA, Davis RE, Lenkinski RE, Wilcott MR (1976) Contact vs. pseudocontact contributions to lanthanide-induced shifts in the nuclear magnetic resonance spectra of isoquinoline and of endo-norbornenol. *J Am Chem Soc* 98:4250–4258
- Taha ZA, Ajlouni AM, Al-Hassan KA, Hijazi AK, Faiq AB (2011) Syntheses, characterization, biological activity and fluorescence properties of bis-(salicylaldehyde)-1, 3-propylenediimine Schiff base ligand and its lanthanide complexes. *Spectrochim Acta A* 81:317–323
- Kai K, Zhang HX, Ma RJ, Chen YN, Chu HB, Zhao YL (2013) Synthesis, characterization and enhanced luminescence of terbium complexes with 2-pyrazinecarboxylic acid and butanedioic acid by inert-fluorescent lanthanide ions. *J Rare Earths* 31:32–36
- Tian L, Ren N, Zhang JJ, Liu HM, Bai JH, Ye HM, Sun SJ (2009) Synthesis, crystal structure, luminescence and thermal decomposition kinetics of Eu (III) complex with 2, 4-dichlorobenzoic acid and 2, 2'-bipyridine. *Inorg Chim Acta* 362:3388–3394

22. Guo DC, He W, Liu B, Gou LN, Li RX (2013) Synthesis and luminescence properties of 2-(benzylcarbamoyl) phenyl derivatives and their europium complexes. *Luminescence* 28: 280–286
23. Kirby AF, Richardson FS (1983) Detailed analysis of the optical absorption and emission spectra of europium ($^{3+}$) in the trigonal (C_3) $\text{Eu}(\text{DBM})_3 \cdot \text{H}_2\text{O}$ system. *J Phys Chem* 87:2544–2556
24. Li WX, Li YJ, Chai WJ, Ren T, Liu Y, Zhang J, Ao BY (2012) Syntheses and fluorescence properties of two novel lanthanide (III) perchlorate complexes with bis (benzylsulfinyl) methane. *J Fluoresc* 22:651–658
25. Guo DC, Wu PL, Tan H, Xia L, Zhou WH (2011) Synthesis and luminescence properties of novel 4-(N-carbazole methyl) benzoyl hydrazone Schiff bases. *J Lumin* 131:1272–1276
26. Ding BD, Zhang JM, Zhu WQ et al (2002) Fast and convenient determination of HOMO energy level of organic electroluminescent material using electrochemistry method. *Chem Res Appl* 14:712–714